Atmos. Chem. Phys., 11, 11647–11655, 2011
www.atmos-chem-phys.net/11/11647/2011/
doi:10.5194/acp-11-11647-2011

Atmospheric Chemistry and Physics

Effects of model resolution on the interpretation of satellite NO_2 observations

L. C. Valin[1], **A. R. Russell**[1], **R. C. Hudman**[1,*], **and R. C. Cohen**[1,2]

[1]College of Chemistry, University of California Berkeley, Berkeley, CA 94720, USA
[2]Department of Earth and Planetary Sciences, University of California Berkeley, Berkeley, CA 94720, USA
[*]now at: Environmental Protection Agency, Region 9, San Francisco, CA 94105, USA

Received: 11 May 2011 – Published in Atmos. Chem. Phys. Discuss.: 18 July 2011
Revised: 2 November 2011 – Accepted: 4 November 2011 – Published: 22 November 2011

Abstract. Inference of NO_x emissions ($NO+NO_2$) from satellite observations of tropospheric NO_2 column requires knowledge of NO_x lifetime, usually provided by chemical transport models (CTMs). However, it is known that species subject to non-linear sources or sinks, such as ozone, are susceptible to biases in coarse-resolution CTMs. Here we compute the resolution-dependent bias in predicted NO_2 column, a quantity relevant to the interpretation of space-based observations. We use 1-D and 2-D models to illustrate the mechanisms responsible for these biases over a range of NO_2 concentrations and model resolutions. We find that predicted biases are largest at coarsest model resolutions with negative biases predicted over large sources and positive biases predicted over small sources. As an example, we use WRF-CHEM to illustrate the resolution necessary to predict 10 AM and 1 PM NO_2 column to 10 and 25 % accuracy over three large sources, the Four Corners power plants in NW New Mexico, Los Angeles, and the San Joaquin Valley in California for a week-long simulation in July 2006. We find that resolution in the range of 4–12 km is sufficient to accurately model nonlinear effects in the NO_2 loss rate.

1 Introduction

NO_x ($NO + NO_2$) is emitted to the troposphere by fossil-fuel combustion, biomass burning, soil microbial processes, and lightning. In the troposphere, NO_x affects ozone production, aerosol formation and atmospheric composition (e.g. CH_4) through feedback on HO_x ($OH + HO_2 + RO_2$). The concentration of OH radical, the main daytime sink of NO_x, depends strongly on NO_x concentration. As a result, the removal rate of NO_x (i.e. $k_{NO_2+OH}[OH]$) depends strongly on its own concentration. Thus, to accurately quantify this removal rate, a model must accurately resolve NO_x from its source (10–100 ppb) to background (10-100 ppt). Column NO_2 (e.g., Heue et al., 2008; Valin et al., 2011) and in situ observations (e.g., Ryerson et al., 2001; Russell et al., 2011) show that this transition can occur at scales as small as 10–20 km, a length scale similar to those reported from calculations (e.g., Cohan et al., 2006; Loughner et al., 2007).

Satellite-based observations of tropospheric NO_2 have provided unique insights into spatial and temporal patterns on regional scales of soil (e.g., Bertram et al., 2005; van der A et al., 2007; Hudman et al., 2010), biomass burning (e.g., Jaegle et al., 2005; Mebust et al., 2011), lightning (e.g., Beirle et al., 2010), and urban NO_x emissions (e.g., Kim et al., 2009; Russell et al., 2010; Beirle et al., 2011). These satellite observations have also provided constraints on inverse models that are used to validate emission inventories (e.g., Martin et al., 2003; Konovalov et al., 2006; Napelenok et al., 2008; Kim et al., 2009). Most of the inverse modeling studies used to validate these emission inventories adjust NO_x emissions with the assumption that model chemistry is accurate. However, errors in our understanding of atmospheric reactions (e.g., Thornton et al., 2002; Mollner et al., 2010) or their representation in models may compromise the accuracy of these inferred emissions. For example, extensive research has demonstrated that modeled ozone production depends strongly on model resolution due to its nonlinear dependence on NO_x concentration (e.g., Sillman et al., 1990; Kumar et al., 1994; Gillani et al., 1996; Cohan et al., 2006; Wild and Prather, 2006). OH, which has the same NO_x-dependence as ozone production, will also vary

Correspondence to: R. C. Cohen
(rccohen@berkeley.edu)

Table 1. Parameters used in HO_x-NO_x steady-state model (Murphy et. al., 2006 and references therein).

Parameter	Value
Initiation	
HO_x Production	0.5×10^7 molecules cm^{-3} s^{-1}
Radical Chain Propagation	
k_{OH+VOC}[VOC]	$1\,s^{-1}$
$k_{RO_2+NO \rightarrow RO+NO_2}$	8×10^{-12} cm^3 molecules^{-1} s^{-1}
Termination	
$k_{RO_2+RO_2-Eff}$	7.5×10^{-12} cm^3 molecules^{-1} s^{-1}
k_{NO_2+OH}	1×10^{-11} cm^3 molecules^{-1} s^{-1}
$k^a_{RO_2+NO \rightarrow RONO_2}$	0×10^{-12} cm^3 molecules^{-1} s^{-1}
$NO_2 : NO_x$	0.7

[a] Alkyl-nitrate formation rate has been set to 0 in these simulations. Increases in this rate will slightly affect NO_x lifetime (Farmer et. al., 2011).

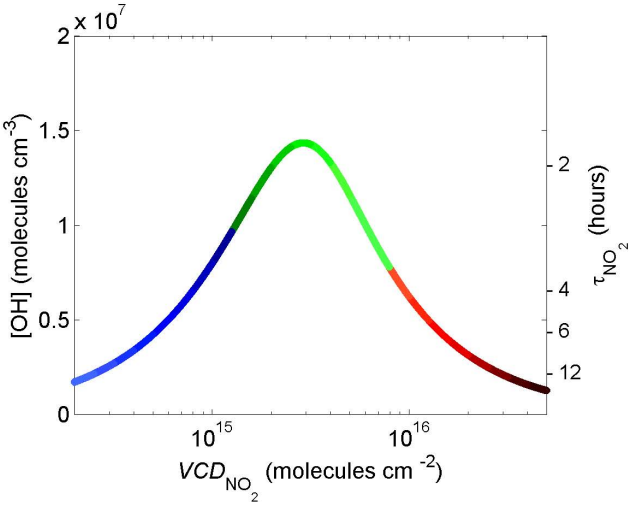

Fig. 1. Steady state OH concentration (left axis) and corresponding NO_2 lifetime $(k_{NO_2+OH} \times OH)^{-1}$ on the right axis versus boundary layer NO_2 column (molecules cm^{-2}) assuming a 1-km well-mixed boundary layer. The color scheme corresponds to regions of high NO_2 (red), where OH is low, intermediate NO_2 (green), where OH is high, and low NO_2 (blue), where OH is low, and is used throughout the article.

with model resolution affecting NO_x lifetime and concentration. As a result, NO_x emissions derived from an inversion of satellite NO_2 observations will have resolution-dependent biases, the magnitude of which is not well known.

We investigate the biases in predicted NO_2 column due to model horizontal resolution. To illustrate the mechanisms at work, we first show how model resolution, OH, and NO_2 interact in 1-D and 2-D plume models. We then use WRF-CHEM, a fully-coupled regional 3-D chemical transport model (CTM), to evaluate the effect in some realistic model situations. We use the simpler models to understand the source of resolution-dependent biases and use WRF-CHEM to determine the model resolution necessary to predict 10 AM and 1 PM column NO_2 to 10 % and 25 % accuracy over the Four Corners and San Juan power plants, the city of Los Angeles, and the San Joaquin Valley in California for a week-long simulation in July 2006.

2 NO_x-OH steady-state chemistry in 1-D and 2-D plume models

Using the analytical solution to the NO_x-HO_x steady-state relationship to determine OH concentration (Table 1) (Murphy et al., 2006 and references therein), we simulate the removal of NO_2 by OH in the outflow of sources using both 1-D and 2-D plume models. The selected chemical parameters are representative of noontime, mid-latitude, NO_x-CH_4-CO chemistry.

Figure 1 shows the dependence of OH on NO_2 derived from this steady-state relationship with the corresponding NO_2 lifetime indicated $(k_{NO_2+OH} \times [OH])^{-1}$. As is well-known, the response of OH to changes in NO_2 depends on NO_2 concentration. For example, decreasing NO_2 at high NO_2 (red) results in an increase of OH and a shorter NO_2 lifetime while at low NO_2 (blue), results in less OH and a longer NO_2 lifetime.

The key feature of this relationship is that the maximum in OH feedback (green) corresponds to a NO_2 lifetime of two hours, an e-folding decay length of 54 km in 5 m s^{-1} winds and of 5–15 km at the slower moving diffusive edges. Poorly resolving these gradients in NO_2 will result in inaccurate OH feedback, biases in NO_2 lifetime, and as a result, modest biases in domain-total NO_2. For resolutions that grossly misrepresent the distribution of NO_2, biases in OH feedback, NO_2 lifetime, and domain-total NO_2 will be massive.

2.1 Biases in a 1-D plume model

In a 1-D model, NO_2 is emitted at the western end of the domain ($x = 0$–1024 km) and transported to the east at a constant rate (5 m/s). We run the model with emission rates of 30, 6.0, and 0.30 kmol h^{-1}. These emission rates are selected to correspond with high, intermediate and low NO_2-OH feedback regimes depicted in Fig. 1. The model is run at east-west resolutions of 0.5 to 512 km with the dimensions perpendicular to the flow fixed at 1 km (north-south and vertical).

When 1-D simulations are run to steady-state, NO_2 is removed by OH such that the spatial gradient reflects the applied NO_2-OH feedback (Fig. 2). Failure to accurately resolve these gradients results in inaccurate OH and biases in both the NO_2 lifetime and concentration. For example, when a large source of NO_2 is computed at 2 km resolution, OH is suppressed so strongly that NO_2 decays by only one

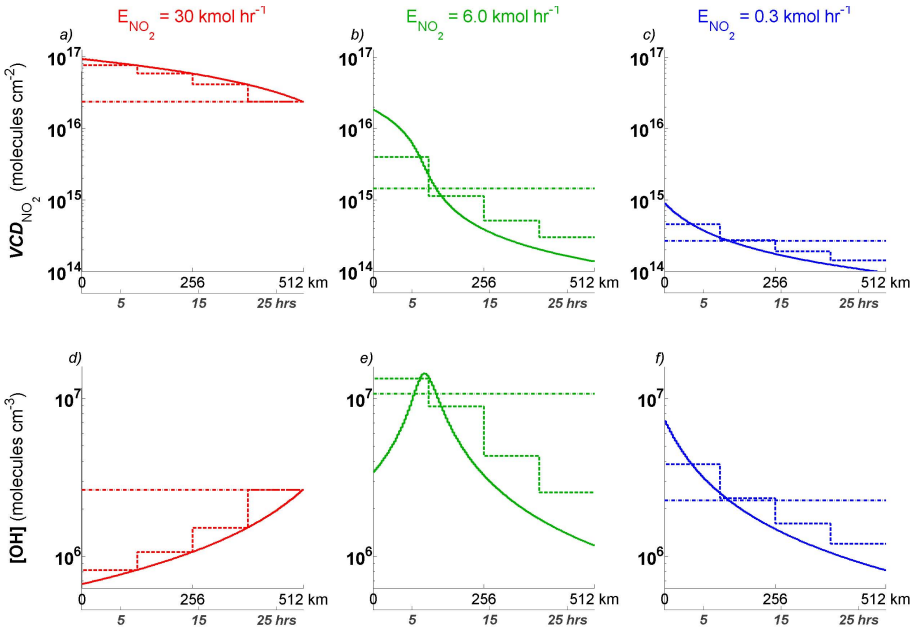

Fig. 2. NO_2 column (molecules cm^{-2}) predicted in a 1-D plume model at 2 km (solid), 128 km (dashed), and 512 km model resolutions (dash-dot) for **(a)** a large, **(b)** intermediate, and **(c)** small source of NO_2 and **(d–f)** the corresponding OH feedback. The color-scheme corresponds to NO_2-OH feedback regimes depicted in Fig. 1. Horizontal (N–S) and vertical layers are fixed at 1 km thickenss for all resolutions.

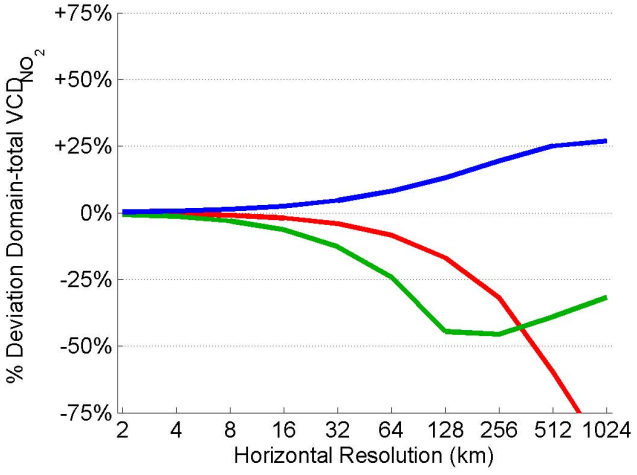

Fig. 3. Resolution-dependent bias in domain-averaged NO_2 column versus model resolution for small (blue), intermediate (green), and large (red) sources of NO_2 in a 1-D plume model (Fig. 2).

e-fold in 400 km, corresponding to a chemical lifetime of 22 h (Fig. 2a, d – solid line). Computed at coarser resolution (128 km), NO_2 is averaged over the entire grid cell such that OH is enhanced, NO_2 is shorter-lived, and NO_2 concentrations are biased low (Fig. 2a, d – dashed line). At this high emission rate, biases in the domain-total NO_2 exceed 50 % at the coarsest resolutions (Fig. 3, red line).

In contrast to a large source, NO_2 emitted from a small source decays rapidly when computed at 2 km resolution, a reflection of high OH concentration (Fig. 2c, f – solid line), but at coarser model resolution (128 km), NO_2 is instantaneously mixed over an entire grid cell resulting in lower OH, a longer NO_2 lifetime, and a corresponding positive bias in domain-total NO_2 concentration (Fig. 2c, f – dashed line, Fig. 3, blue line).

For an intermediate source of NO_2, the plume decays by an e-fold within 60 km at 2 km model resolution, a gradient corresponding to a chemical lifetime of about three hours and near-maximum OH (Fig. 2b, e – solid line). Model calculations at coarser resolutions (128 km) are not capable of resolving this sharp gradient. Because NO_2 concentrations predicted for an intermediate source are near the maximum OH (Fig. 1, green), biases behave like those of a large source at finer model resolutions and like those of a small source at coarser resolutions (Fig. 3, green line).

In a 1-D model, domain-averaged NO_2 predicted at coarse resolutions is biased (Fig. 3). At intermediate resolutions the biases are moderate (10–30 %) and result from numerical resolution that dilute NO_2 at the leading edge of the plume and shift OH to the left in Fig. 1. When the model resolution becomes much larger than the plume itself, OH feedbacks are shifted by a factor 2-5 times that of the plume simulated in a resolved calculation (e.g., Fig. 2a, d) and gross biases in domain-total NO_2 are predicted (>50 %, Fig. 3).

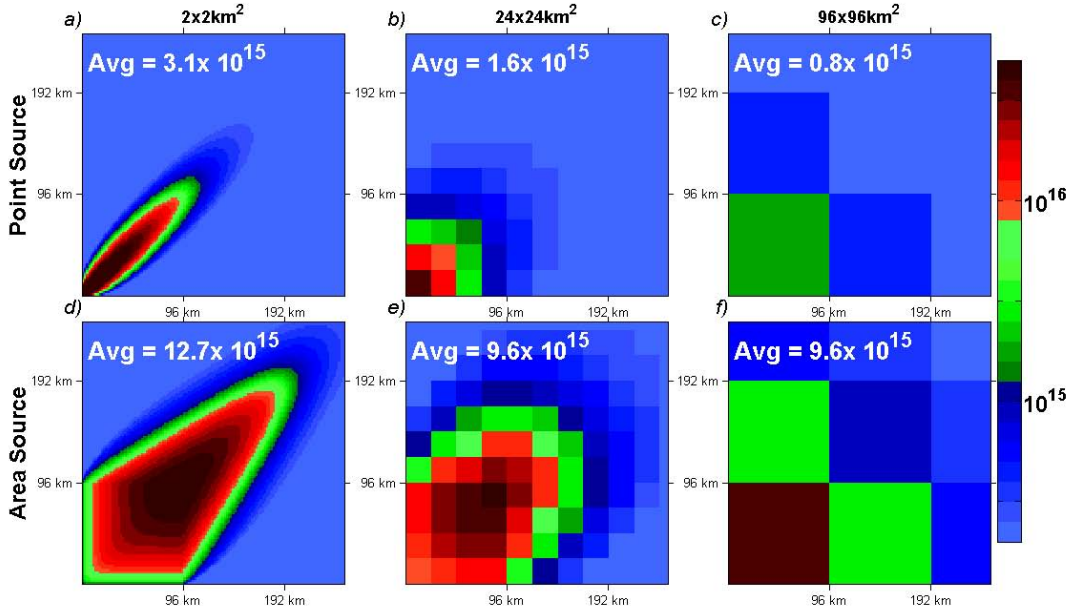

Fig. 4. NO_2 column (molecules cm^{-2}) predicted in a 2-D plume model for a large point source simulated at **(a)** 2 km, **(b)** 24 km, and **(c)** 96 km resolution, and the same for simulation of a large area source **(d–f)**. The color-scheme corresponds to NO_2-OH feedback regimes depicted in Fig. 1. The vertical layer is fixed at 1 km thickness for all simulations shown.

2.2 Biases in a 2-D plume model

While 1-D models are illustrative, 2-D models are a better approximation of NO_2 column and provide some additional insights. For instance, we can consider the effects of horizontal diffusion as well as different source distributions. In this 2-D model, we define a point source (2×2 km^2) with emission rates of 200, 40, and 2 kmol h^{-1} and an area source (96×96 km^2) with emission rates of 1000, 200, and 10 kmol h^{-1} both located in the far southwest corner ($x = y = 0$ km) of the domain ($x = y = 0$–384 km). These emission rates are selected so that the simulated plume concentration corresponds with the high, intermediate and low NO_2-OH feedback regimes depicted in Fig. 1. In this model, NO_2 is transported with x and y wind speeds of 3 m s^{-1}, a mean flow of $3\sqrt{2}$ m s^{-1} to the northeast. Diffusion rates are set to 10 m^2 s^{-1}. Initial and horizontal boundary concentrations are set to 0.5 ppt. The model is computed at six grid resolutions (2, 4, 12, 24, 48, and 96 km), with the vertical layer fixed at 1 km. We run simulations of NO_2 with OH determined by the steady state equation (Table 1, Fig. 1).

When the 2-D model is run to steady-state, a large point source of NO_2 is OH suppressing and long-lived when simulated at 2 km model resolution, but experiences high OH and is short-lived when simulated at coarse resolution (96 km) (Fig. 4a–c). Because the resolved plume is so narrow ($\sim24\sqrt{2}$ km, Fig. 4a), the distribution of NO_2 and the corresponding OH feedbacks are grossly mis-predicted at 96 km resolution with biases in domain-averaged NO_2 as high as 75 % (Fig. 5b). Over a small source (*not shown*), the opposite effect occurs in a model; a small source is OH-enhancing and short-lived at 2 km resolution, but experiences low OH and is long-lived at coarser resolutions. As a result, domain-averaged NO_2 predicted over a small source is biased 100 %.

When the same 2-D model is run to steady-state using emissions from an area source (Fig. 4d–f), domain-averaged biases in NO_2 are relatively modest ($\sim$25 % at 96 km model resolution) but follow the same general pattern as those simulated over a point source (Fig. 5). The biases predicted over an area source are smaller because coarse model resolutions are better able to characterize the distribution of NO_2 and corresponding OH feedbacks over the simulated plume, which is much wider than that predicted over a point source. From previous discussion, it would be expected that simulation of NO_2 at 96 km model resolution would be massively biased since the resolved plume is approximately 96 km wide. However, the alignment of this area source (96×96 km^2) on this 96-km grid results in an NO_2 distribution that roughly approximates that simulated in a resolved model, resulting in biases that are relatively small ($\sim$25 %). When the 96×96 km^2 area source is shifted by 48 km and evenly distributed over four 96 km grid cells (*not shown*), biases predicted at 96 km resolution are as large as those predicted for a point source (>75 %).

Figure 5 summarizes biases predicted in a 2-D model as a function of model resolution, source strength, and proximity to the source. Biases predicted for NO_2 in a constant OH field (OH = 5.5×10^6 molecules cm^3), that is without any NO_2-OH feedback and only subject to transport effects (Fig. 5b–e, black line), are negligible over the entire

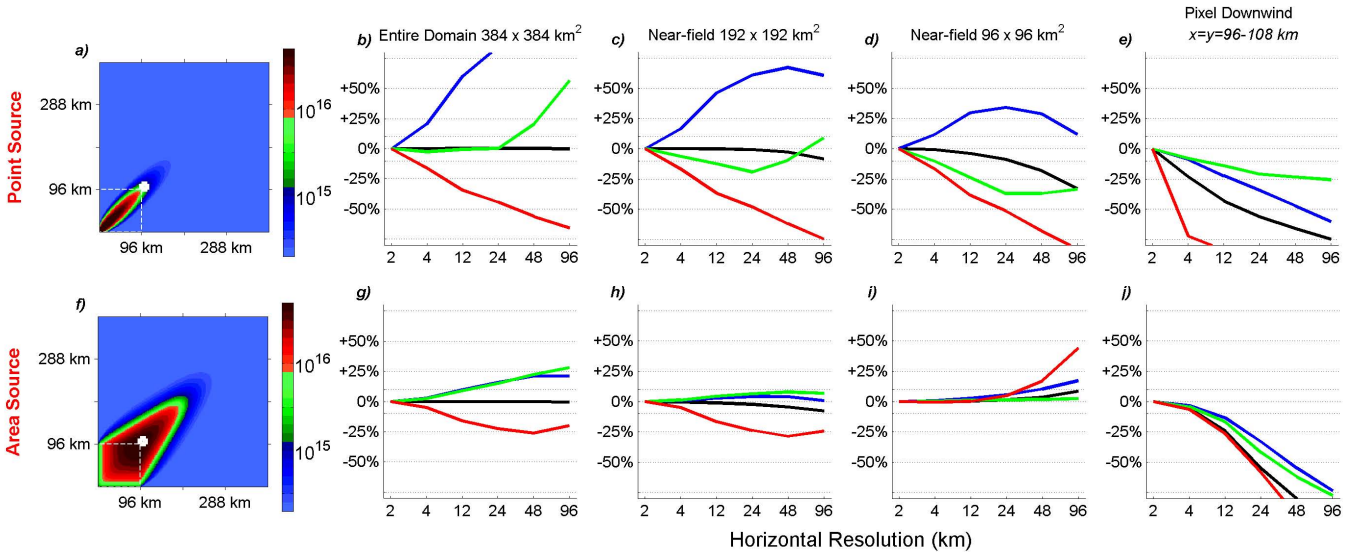

Fig. 5. (a) NO_2 column (molecules cm^{-2}) predicted in a 2-D plume model for a large point source simulated at 2 km resolution with vertical layer fixed at 1 km thickness. Resolution-dependent bias in domain-averaged NO_2 column over the **(b)** entire domain ($x = y = 0$–384 km), **(c)** the 192 km near-field ($x = y = 0$–192 km), **(d)** the 96 km near-field ($x = y = 0$–96 km), and **(e)** at a pixel downwind ($x = y = 96$–108) for NO_2 emitted from a large (red), an intermediate (green), and a small (blue) point source of NO_2 with OH = f_{NO_2} as in Fig. 1 and from a large point source with OH set to 5×10^6 molecules cm^{-3} (black). **(f–j)** The same for simulation of a 96×96 km^2 area source.

domain (∼0 %, 5b), significant over the 192 km nearest the source (−10 %, 5c), and large in both the 96 km nearest the source (−30 %, 5d) and in a 12×12 km^2 pixel 96 km downwind from the source (−75 %, 5e). Without OH feedback, these biases are due to numerical artifacts in computing a short-lived species on a coarse grid, but are are negligible over regions that are large (e.g., 192 km) compared to the spatial scale of chemical decay (e-fold decay over 84 km) (e.g., Fig. 5c, black). When subject to NO_2-OH chemical feedbacks (Fig. 5b–e, red, green, and blue lines), biases diverge from that of transport alone (black) with behavior depending, as expected, on the rate of NO_x emissions. Over each spatial domain considered, simulation of a large source (red) is biased low versus transport alone (black) whereas the opposite is true for a small source (blue). For both large and small sources, the magnitude of the bias increases as the model resolution coarsens. In both the point and area source examples, the behavior of biases depends on model resolution.

VOC reactivity affects predicted biases by altering the NO_2 concentration at which maximum OH occurs (Fig. 1, Table 1). For simulations with VOC reactivity increased by a factor of 10 and the same NO_2 emissions, we find that the pattern of predicted biases changes in the direction one expects based on the shifts in the NO_2-OH relationship for an increase in VOC. However, if the NO_x emission rates are increased along with VOC reactivity, the patterns of biases returns to those predicted at the original VOC conditions.

Biases in a 2-D model are predicted to be unacceptably large (up to ∼75–100 %) at relevant horizontal resolutions (96 km) with behavior that depends dramatically on source strength (+100 % for small source to −75 % for large source) and distribution (∼ 75 % for point source to ∼ 25-75 % for area source). Biases predicted in a 2-D model are much larger than those predicted at the same model resolution in a 1-D model because the plume can diffuse horizontally. However, the basic resolution dependent effects are the same – numerical dilution shifts the NO_x-OH feedback to the left on Figure 1, altering the spatial pattern of NO_2 from a resolved calculation. These effects are modest (0–30 %) if the model resolution is finer than the width of a fully-resolved plume, but are massive (>50 %) if the resolution is comparable to or larger than the plume (Figs. 4, 5).

3 Illustration of effects in WRF-CHEM: Four Corners, Los Angeles, and San Joaquin Valley

Regional CTMs, like WRF-CHEM (Grell et al., 2005), provide a realistic and fully-coupled description of atmospheric mixing, chemistry, and emissions. We use WRF-CHEM to test for resolution-dependent biases over three distinct source regions: the Four Corners Power Plants, Los Angeles, and the San Joaquin Valley. Air quality control strategies often use 10 or 25 % NO_x reductions as a realistic regulatory benchmark. Using WRF-CHEM, we simulate the 10 AM and 1 PM NO_2 column, as would be observed by space-based

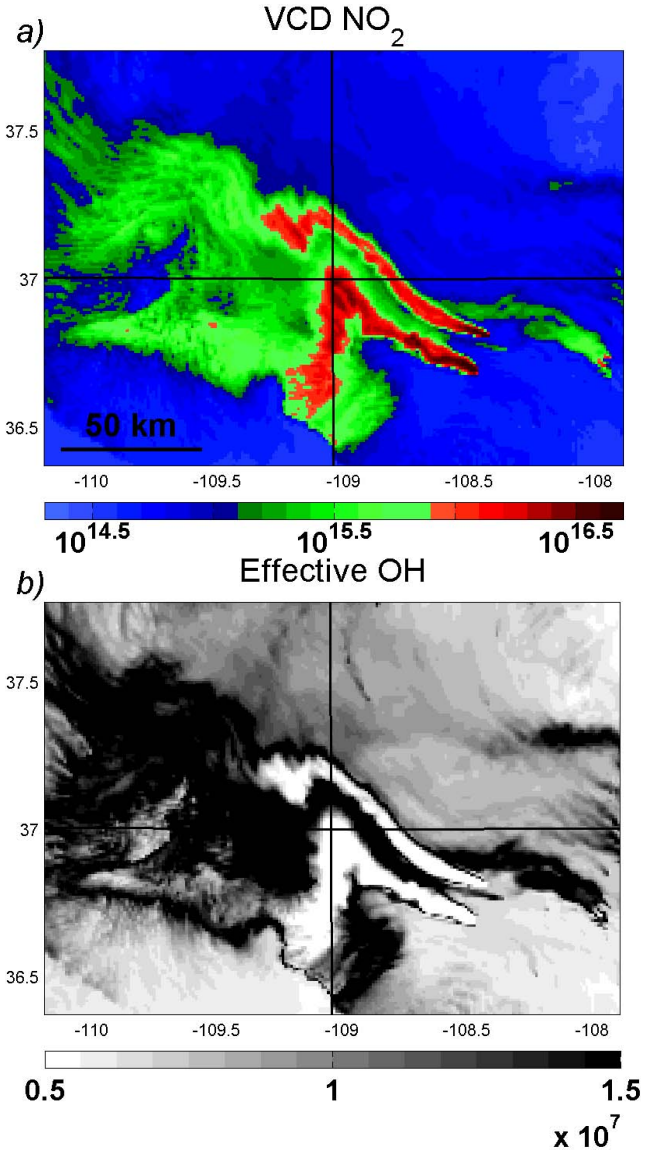

Fig. 6. **(a)** NO_2 column (molecules cm^{-2}) and **(b)** effective OH, or the NO_2-weighted average of OH (molecule cm^{-3}), taken over the entire vertical column as simulated with WRF-CHEM at 1 km resolution over the Four Corners Region of US at 10 a.m. on 5 July 2006.

UV/VIS instruments, over the Four Corners and San Juan Power Plants in Northwest New Mexico (185 kmol h^{-1}) at 1, 4, 12, and 24 km resolution and over California, which includes the Los Angeles Basin (1020 kmol h^{-1}) and the San Joaquin Valley (410 kmol h^{-1}) at 4, 12, 24, 48, and 96 km resolution to examine the grid resolution necessary to attain 10 % and 25 % accuracy for a 1-7 July 2006 simulation. For a more detailed description of the WRF-CHEM simulations see the Appendix.

Four Corners, Los Angeles and the San Joaquin Valley are large enough sources of NO_x such that OH is suppressed in a resolved simulation. For example, effective OH, or the NO_2-weighted OH concenntration that is simulated at 1 km resolution over Four Corners is low ($<5 \times 10^6$ molecules cm^{-3}) where NO_2 concentration is high (Fig. 6a–b, red), enhanced ($>1.5 \times 10^7$ molecules cm^{-3}) where NO_2 is intermediate (Fig. 6a-b, green) and low ($\sim 5 \times 10^6$ molecules cm^{-3}) where NO_2 is low (Fig. 6a–b, blue). At coarser resolutions, NO_2 is numerically diluted, and prediction of NO_2 column is biased low just as was predicted over large sources in the 1-D and 2-D plume models. Over Four Corners, the 1 PM NO_2 column simulated at 24 km is biased −50 % relative to simulation at 1 km (Fig. 7). Over Los Angeles, the 1 PM NO_2 column is biased −13 % at 24 km resolution relative to simulation at 4 km, but is biased −37 % at 96 km resolution (Fig. 8). Over the San Joaquin Valley, the biases relative to 4 km simulation are −16 % at 12 km resolution, −24 % at 24 km resolution and −36 % at 48 km resolution (Fig. 9). We find that the exact numbers depend on the choice of the boundaries that surround each plume, but that the conclusions are independent of that choice. As a result of these biases, prediction of the domain-averaged NO_2 column to 25 % accuracy at 1 PM requires model resolution of 4 km over Four Corners, 12 km over San Joaquin Valley, and 48 km over Los Angeles under the conditions tested here. For 10 % accuracy, 4 km model resolution is required over Four Corners and the San Joaquin Valley while 12 km resolution is sufficient over Los Angeles.

Biases in NO_2 column at 10 AM (*not shown*) are consistently smaller than those predicted at 1 PM because the NO_2 column predicted at 10 AM is exposed to much less OH through the nighttime and early morning hours. As a result, prediction of 10 AM NO_2 column to 25 % accuracy as tested here requires slightly coarser model resolution than was necessary at 1 PM: 12 km over Four Corners, 24 km over San Joaquin Valley, and 48 km over Los Angeles. For 10 % accuracy, model resolution of 4 km is necessary over Four Corners, 24 km over San Joaquin Valley and 48 km over Los Angeles.

All three of these regions are biased low at coarse model resolutions (Figs. 7–9), which is expected for large, OH-suppressing sources of NO_x. For Los Angeles and Four Corners, sources that are directly comparable to the large 2-D area and point sources, biases behave similarly to those predicted in the 2-D plume model. And while the San Joaquin Valley appears to be an intermediate source of NO_x (Fig. 9), which according to the 2-D plume model would indicate that coarse resolution prediction of NO_2 should be biased high (Fig. 5h), it is important to consider the differences between the 2-D plume model, which simulates midday summertime chemistry at steady-state, with WRF-CHEM, which integrates the full diurnal cycle. In WRF-CHEM, all of these sources (Figs. 7–9), including the San Joaquin Valley, suppress OH through the morning hours when NO_x concentrations are higher and HO_x production rate is lower, leading to

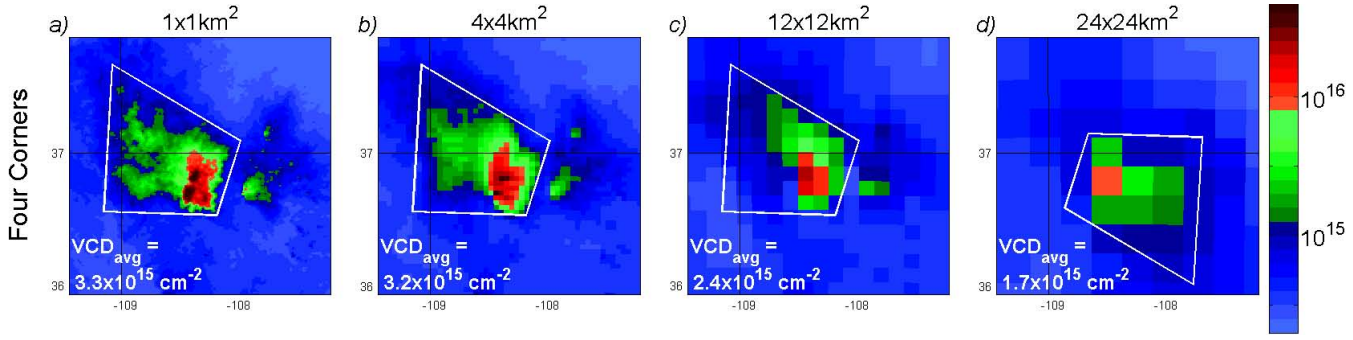

Fig. 7. WRF-CHEM 3–7 July 2006, 1 p.m. LST average NO_2 column (molecules cm^{-2}) simulated over Four Corners Region of US at **(a)** 1 km, **(b)** 4 km, **(c)** 12 km, and **(d)** 24 km model resolution. NO_2 column is averaged over a sub-domain (white box) and reported in the bottom left corner of each panel. The sub-domain in the 24 km simulation was rotated to include the plume, which was predicted further to the SE than those predicted at 1, 4, or 12 km resolution.

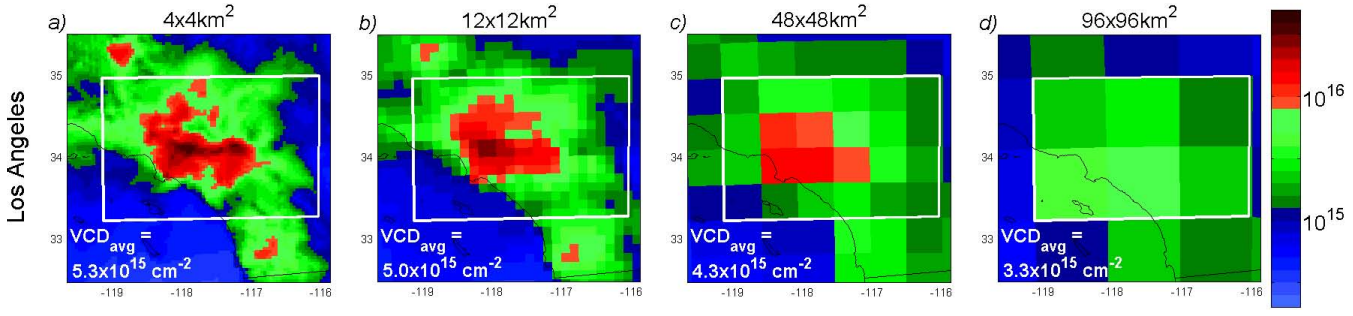

Fig. 8. WRF-CHEM 3–7 July 2006, 1 p.m. LST average NO_2 column (molecules cm^{-2}) simulated over Los Angeles at **(a)** 4 km, **(b)** 12 km, **(c)** 48 km, and **(d)** 96 km model resolution. NO_2 column is averaged over a sub-domain (white box) and reported at the bottom of each panel.

biases that start small in the morning hours and grow with time of day.

4 Implications for interpretation of satellite observations

The calculations above show that predicted NO_2 columns will depend on the resolution of the model. As a consequence, any inference of NO_x emissions that relies on a model to interpret satellite observations will have biases if the model resolution is too coarse. The calculations above show that the biases are both positive and negative as a result of the interplay of NO_2 and OH. We find that predicted biases are especially large where steep gradients of NO_2 dominate the total NO_2 mass (e.g. 2-D point source) and that they are are smaller where shallow gradients dominate the total NO_2 mass (e.g. 2-D area source). In general, gradients are shallow where NO_x lifetime is long compared to transport timescales (e.g. wintertime, morning hours) and are steep where NO_x lifetime is short compared to the timescale of transport (e.g. summertime, afternoon hours).

For situations presented here, model resolution in the range of 4–12 km is sufficient to predict the effects of NO_2-OH feedbacks on the NO_2 lifetime and column to 10 % accuracy. This value will change depending on the location, season, and time of day according to general guidelines provided above. Nonetheless our analysis suggests that numerical resolution needs to be small compared to the NO_x e-folding distance. A growing set of observations over both power plants and urban sources at different times of year indicate that boundary layer NO_x often exhibit e-folding distances of order 10–30 km (e.g, Ryerson et al., 2001; Loughner et al., 2007; Heue et al., 2008; Russell et al., 2011; Valin et al., 2011) supporting the idea that model resolution in the range of 4-12 km is necessary in a broad range of contexts. For any calculation where accurate computation of boundary layer NO_x is important we recommend model calculations to test whether the spatial resolution is sufficient to calculate NO_2 to the desired accuracy.

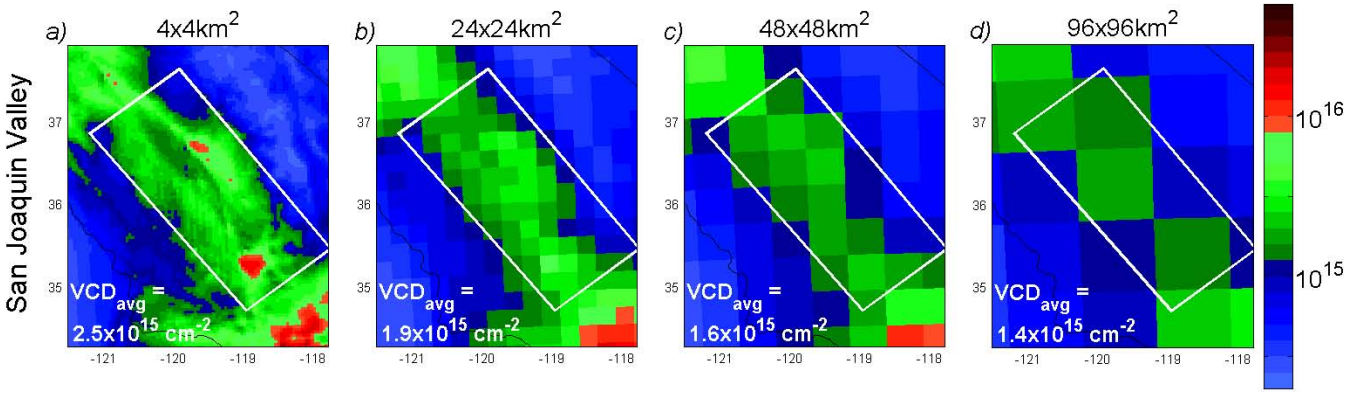

Fig. 9. WRF-CHEM 3–7 July 2006, 1 p.m. LST average NO_2 column (molecules cm^{-2}) over the San Joaquin Valley at **(a)** 4 km, **(b)** 12 km, **(c)** 24 km, and **(d)** 48 km model resolution. NO_2 column is averaged over a sub-domain (white box) and reported at the bottom of each panel.

5 Conclusions

We investigate the effects of NO_2-OH chemical feedbacks on predicted NO_2 in a 1-D plume model, a 2-D plume model, and WRF-CHEM, a fully-coupled 3-D CTM. We use 1-D and 2-D plume models to demonstrate that nonlinear NO_2-OH chemical feedback leads to biases in column NO_2. As a result, inference of NO_x emission inventories from chemical transport models will suffer biases that depend on the horizontal resolution of the model. Using WRF-CHEM, we determine the model resolution necessary to predict NO_2 column to 10 % and 25 % accuracy over Los Angeles, the San Joaquin Valley, and Four Corners for a week-long simulation in July 2006. In this example, we find that prediction of NO_2 column to 10 % accuracy at 1 PM requires model resolution of 4 km over both Four Corners and the San Joaquin Valley while 12 km is sufficient over Los Angeles. Prediction to 10 % accuracy at 10 AM requires model resolution of 4 km over Four Corners, 24 km over San Joaquin Valley, and 48 km over Los Angeles. In these examples, we find that model resolution must be comparable to, or smaller than, the spatial variability of NO_2 to accurately model NO_2-OH feedbacks on NO_2 column. Thus, simulations aimed at matching satellite observations must be run at sufficient spatial resolution to avoid contamination by numerical artifacts.

Appendix A

We simulate column NO_2 from 1–7 July 2006, over California, Nevada, Northern Mexico, and the Eastern Pacific centered over Southern California ($2304 \times 2304\,km^2$) at 4, 12, 24, 48, and 96 km resolution. The simulated domain is much larger than the region of interest to ensure that there are no effects of boundary conditions in the coarser resolution model simulations. The first two days of simulation are used as spin-up, and the last five days (3–7 July) are averaged to 1 p.m. LST for all analyses. Emissions are the National Emission Inventory (NEI) 2005 on-road and off-road transportation emissions for a typical July weekday and Continuous Emissions Monitoring (CEMS) averaged point source emissions for a typical August, 2006, weekday. For more information, see ftp://aftp.fsl.noaa.gov/divisions/taq/emissions_data_2005/Weekday_emissions/readme.txt. Biogenic emissions for all model resolutions were generated by an online module as in (Grell et al., 2005) at 4 km horizontal resolution for a single July day and kept constant throughout the 7-day simulation. We use the Regional Acid Deposition Model, version 2 chemical mechanism (Stockwell et al., 1990). The initial and boundary chemical conditions are derived from idealized profiles that are standard in WRF-CHEM. Radiative feedback from clouds on photolysis rates was disabled in order to simulate column NO_2 under clear-sky conditions that are typical of satellite observations. Meteorological initial and boundary conditions for the simulation are derived from the North American Regional Reanalysis for July 2005 (NARR – http://nomads.ncdc.noaa.gov/dods/NCEP_NARR_DAILY).

We simulate column NO_2 over the Four Corners region in the Western US ($384 \times 384\,km^2$) at 1, 4, and 12 km resolution and extend the boundaries ($1536 \times 1536\,km^2$) to simulate the same domain at 24 km resolution. This domain is centered on the Four Corners and San Juan Power Plants, which are approximately 20 km apart. This simulation is run in the same manner as that run over California except that only emissions from point sources are included. For simulation at 24 km resolution, as mentioned, the domain is extended to avoid boundary relaxation effects that occur over the 5 boundary grid cells in WRF-CHEM.

Acknowledgements. This work was supported by CARB under Grant #06-328, NASA under Grant #NNX08AE566, and by NASA Headquarters under the NASA Earth and Space Science Fellowship Program – Grant NESSF09.

Edited by: P. Jöckel

References

Beirle, S., Huntrieser, H., and Wagner, T.: Direct satellite observation of lightning-produced NO_x, Atmos. Chem. Phys., 10, 10965–10986, doi:10.5194/acp-10-10965-2010, 2010.

Beirle, S., Boersma, K. F., Platt, U., Lawrence, M. G., and Wagner, T.: Megacity emissions and lifetimes of nitrogen oxides probed from space, Science, 333, 1737–1739, doi:10.1126/science.1207824, 2011.

Bertram, T. H., Heckel, A., Richter, A., Burrows, J. P., and Cohen, R. C.: Satellite measurements of daily variations in soil NO_x emissions, Geophys. Res. Lett., 32, L24812, doi:10.1029/2005GL024640, 2005.

Cohan, D. S., Hu, Y., and Russell, A. G.: Dependence of ozone sensitivity analysis on grid resolution, Atmos. Env., 40, 126–135, doi:10.1016/j.atmosenv.2005.09.031, 2006.

Farmer, D. K., Perring, A. E., Wooldridge, P. J., Blake, D. R., Baker, A., Meinardi, S., Huey, L. G., Tanner, D., Vargas, O., and Cohen, R. C.: Impact of organic nitrates on urban ozone production, Atmos. Chem. Phys., 11, 4085–4094, doi:10.5194/acp-11-4085-2011, 2011

Gillani, N. V., and Pleim, J. E.: Sub-grid-scale features of anthropogenic emissions of NO_x and VOC in the context of regional Eulerian models, Atmos. Environ., 30, 2043-2059, doi:10.1016/1352-2310(95)00201-4,1996.

Grell, G. A., Peckham, S. E., Schmitz, R., McKeen, S. A., Frost, G., Skamarock, W. C., and Eder, B.: Fully coupled "online" chemistry within the WRF model, Atmos. Environ., 39, 6957–6975, 2005.

Heue, K.-P., Wagner, T., Broccardo, S. P., Walter, D., Piketh, S. J., Ross, K. E., Beirle, S., and Platt, U.: Direct observation of two dimensional trace gas distributions with an airborne Imaging DOAS instrument, Atmos. Chem. Phys., 8, 6707–6717, doi:10.5194/acp-8-6707-2008, 2008.

Hudman, R. C., Russell, A. R., Valin, L. C., and Cohen, R. C.: Interannual variability in soil nitric oxide emissions over the United States as viewed from space, Atmos. Chem. Phys., 10, 9943–9952, doi:10.5194/acp-10-9943-2010, 2010.

Jaegle, L., Steinberger, L., Martin, R. V., and Chance, K.: Global partitioning of NO_x sources using satellite observations: Relative roles of fossil fuel combustion, biomass burning and soil emissions, Faraday Discussions, 130, 407–423, doi:10.1039/b502128f, 2005.

Kim, S. W., Heckel, A., McKeen, S. A., Frost, G. J., Hsie, E. Y., Trainer, M. K., Richter, A., Burrows, J. P., Peckham, S. E., and Grell, G. A.: Satellite-observed US power plant NO_x emission reductions and their impact on air quality, Geophys. Res. Lett., 33, L22812, doi:10.1029/2006gl027749, 2006.

Konovalov, I. B., Beekmann, M., Richter, A., and Burrows, J. P.: Inverse modelling of the spatial distribution of NO_x emissions on a continental scale using satellite data, Atmos. Chem. Phys., 6, 1747–1770, doi:10.5194/acp-6-1747-2006, 2006.

Kumar, N., Odman, M. T., and Russell, A. G.: Multiscale air quality modeling: Application to Southern California, J. Geophys. Res.-Atmos., 99, 5385–5397, 1994.

Loughner, C. P., Lary, D. J., Sparling, L. C., Cohen, R. C., DeCola, P., and Stockwell, W. R.: A method to determine the spatial resolution required to observe air quality from space, IEEE Trans. Geosci. Remote Sens., 45, 1308–1314, doi:10.1109/tgrs.2007.893732 , 2007.

Martin, R. V., Jacob, D. J., Chance, K., Kurosu, T. P., Palmer, P. I., and Evans, M. J.: Global inventory of nitrogen oxide emissions constrained by space-based observations of NO_2 columns, J. Geophys. Res.-Atmos., 108, 4537, doi: 10.1029/2003JD003453, 2003.

Mebust, A. K., Russell, A. R., Hudman, R. C., Valin, L. C., and Cohen, R. C.: Characterization of wildfire NO_x emissions using MODIS fire radiative power and OMI tropospheric NO_2 columns, Atmos. Chem. Phys., 11, 5839–5851, doi:10.5194/acp-11-5839-2011, 2011

Mollner, A. K., Valluvadasan, S., Feng, L., Sprague, M. K., Okumura, M., Milligan, D. B., Bloss, W. J., Sander, S. P., Martien, P. T., Harley, R. A., McCoy, A. B., and Carter, W. P. L.: Rate of gas phase association of hydroxyl radical and nitrogen dioxide, Science, 330, 646–649, doi:10.1126/science.1193030, 2010.

Murphy, J. G., Day, D. A., Cleary, P. A., Wooldridge, P. J., Millet, D. B., Goldstein, A. H., and Cohen, R. C.: The weekend effect within and downwind of Sacramento: Part 2. Observational evidence for chemical and dynamical contributions, Atmos. Chem. Phys. Discuss., 6, 11971–12019, doi:10.5194/acpd-6-11971-2006, 2006.

Napelenok, S. L., Pinder, R. W., Gilliland, A. B., and Martin, R. V.: A method for evaluating spatially-resolved NO_x emissions using Kalman filter inversion, direct sensitivities, and space-based NO_2 observations, Atmos. Chem. Phys., 8, 5603–5614, doi:10.5194/acp-8-5603-2008, 2008.

Russell, A. R., Valin, L. C., Bucsela, E. J., Wenig, M. O., and Cohen, R. C.: Space-based constraints on spatial and temporal patterns of NO_x emissions in California, 2005–2008, Environ. Sci. Technol., 44, 3608–3615, doi:10.1021/es903451j, 2010.

Sillman, S., Logan, J. A., and Wofsy, S. C.: A regional scale-model for ozone in the United States with subgrid representation of urban and power-plant plumes, J. Geophys. Res.-Atmos., 95, 5731–5748, 1990.

Stockwell, W. R., Middleton, P., Chang, J. S., and Tang, X. Y.: The 2nd generation Regional Acid Deposition Model chemical mechanism for regional air-quality modeling, J. Geophys. Res.-Atmos., 95, 16343–16367, 1990.

Thornton, J. A., Wooldridge, P. J., Cohen, R. C., Martinez, M., Harder, H., Brune, W. H., Williams, E. J., Roberts, J. M., Fehsenfeld, F. C., Hall, S. R., Shetter, R. E., Wert, B. P., and Fried, A.: Ozone production rates as a function of NO_x abundances and HO_x production rates in the Nashville urban plume, J. Geophys. Res.-Atmos., 107, 4146, doi:10.1029/2001jd000932, 2002.

Valin, L. C., Russell, A. R., Bucsela, E. J., Veefkind, J. P., and Cohen, R. C.: Observation of slant column NO_2 using the super-zoom mode of AURA-OMI, Atmos. Meas. Tech., 4, 1929–1935, doi:10.5194/amt-4-1929-2011, 2011.

van der A, R. J., Eskes, H. J., Boersma, K. F., vanNoije, T., Van-Roozendael, M., De Smedt, I., Peters, D. H. M. U. and Meijer, E. W., Trends, seasonal variability and dominant NO_x source derived from a ten year record of NO_2 measured from space, J. Geophys. Res., 113, D04302, doi:10.1029/2007JD009021, 2008

Wild, O. and Prather, M. J.: Global tropospheric ozone modeling: quantifying errors due to grid resolution, J. Geophys. Res.-Atmos., 111, D11305, doi:10.1029/2005jd006605, 2006.